International Journal of Cast Metals Research

Research article

title page;

Stephanie Duwe*[a], Martin Liepe[b], Martin Schrumpf[c], Babette Tonn[a], Rüdiger Bähr[b]

Martin.Liepe@ovgu.de, Stephanie.Duwe@tu-clausthal.de (ORCID 0000-0002-2119-3716), Dr.M.Schrumpf@walzenqlb.de, Babette.Tonn@tu-clausthal.de (ORCID 0000-0003-1467-9213), Ruediger.Baehr@ovgu.de

*corresponding author

[a]Clausthal University of Technology – Institute of Metallurgy
Robert-Koch-Str. 42, 38678 Clausthal-Zellerfeld, Germany

[b]Otto von Guericke University Magdeburg – Institute of Manufacturing Technology and Quality Management
Universitätsplatz 2, 39106 Magdeburg, Germany

[c]Walzengiesserei & Hartgusswerk Quedlinburg
Klopstockweg 33, 06484 Quedlinburg

abstract (150 words)

For manufacturing of steel wires, tubes, and profiles in hot rolling mills the toughest conditions occur in the front rolling stands where the mechanical load comes along with a constant change of hot rolling stock and cooling liquid. Conventional roll materials as pearlitic or acicular cast irons are not able to overcome these intense conditions because of their lack of ductility. A fine selection of alloying elements leads to a new material with a microstructure uniting bainite, austenite, and martensite inducing high hardness and strength, without lacking elongation. For this purpose, a full-factorial design of experiments was created consisting of three alloying elements in two concentrations each. The alloys were cast, heat-treated, and underwent extensive investigations on mechanical properties and microstructure. The results were analyzed and implemented in mathematical models whose combination and optimization led to the identification of the ideal alloy meeting the required strength, hardness, and elongation.

keywords (8)

ductile iron, wear resistant, rolling application, alloy design, design of experiments, process simulation, microstructure

A new ductile iron for mechanically and thermally strained rolls
Part 2: Material development varying Ni, Mo, Cr content using DoE

1 Motivation

Conventional wear resistant cast iron with a matrix of primary cementite, pearlite and other primary carbides cannot stand the service in the first roll stands of hot rolling mills for wires, pipes, or sections. The challenges to be faced are high thermal and mechanical dynamic loads combined with abrasive wear that yield early failure.

The aim was to develop a material based on cast iron with nodular graphite for the manufacture of rolls with the required mechanical properties, in particular sufficient elongation at break in combination with high hardness and yield strength. A heat treatment specifically adjusted to the target material and the use of carefully chosen alloying elements yield the formation of favored microstructure and corresponding properties to produce highly qualified cast iron for rolls.

The choice of a bainite-based ductile iron for rolls is essential as it shows an excellent combination of mechanical strength and wear resistance [1]. The hardness and compressive strength of the bainite ductile iron reach high levels and the impact wear resistance of the bainite ductile iron is twice that of steel [2]. The microstructure of these rolls is full of phases and constituents that all have different purposes. Only together they can face the extreme and alternating mechanical and thermal loads. By the use of well thought out heat treatment, a microstructure of bainite, austenite, and martensite (BAM) is the ultimate target that provides the material behavior needed:

- First, there is the *graphite*. It should be spherical, i.e., the nodularity should be greater than 80 %. It provides a base ductility, good machinability and serves as carbon sink and source during matrix evolution.

- The base of matrix evolution is *austenite*. It should be finely grained with a homogenous element distribution. It sets the course of ferrite and Fe_3C development in bainite transformation. A small amount of retained austenite gives additional ductility. But attention needs to be paid, as it is not stabilized, there is a chance it turns into martensite when set under load which can lead to spontaneous brittle failure of the material.

- During cooling, the main part of the austenitic matrix is ideally transformed to *bainite*, a multiphase structure composed of ferrite needles surrounded by or suffused with Fe_3C carbides depending on the heat treatment applied. A very good and detailed introduction is provided by Lünenbürger [3]. Bainite generates a proper material strength that can compete with that of a steel accompanied by a comfortable ductility – a combination perfectly adapted to changing stresses and strains.

- For obtaining the final dram of strength a small portion of *martensite* is desired as a support for the bainite, just enough to enhance the material's strength and hardness without becoming brittle.

- In addition, wear is a factor that must not be underestimated. To face the abrasion caused by the hot rolling stock a sufficient number of *carbides* needs to be incorporated into the matrix – also a part where martensite is beneficial: it anchors the outstretching primary carbides to the matrix [4].

- *Pearlite* provides strength to the material but at the expense of ductility. So, the amount of pearlite should be kept at low level – not more than around 10 % of the matrix.

This list of partly opposing specifications can only be accomplished by careful alloying and cooling strategies.

As an example, the microstructure of a reference material is depicted in Figure 1. The sample was taken from a roll made of ductile iron with all the ingredients listed above that nevertheless broke while operating in one of the first stands of a hot rolling mill. This serves as the base on which the new alloy is developed.

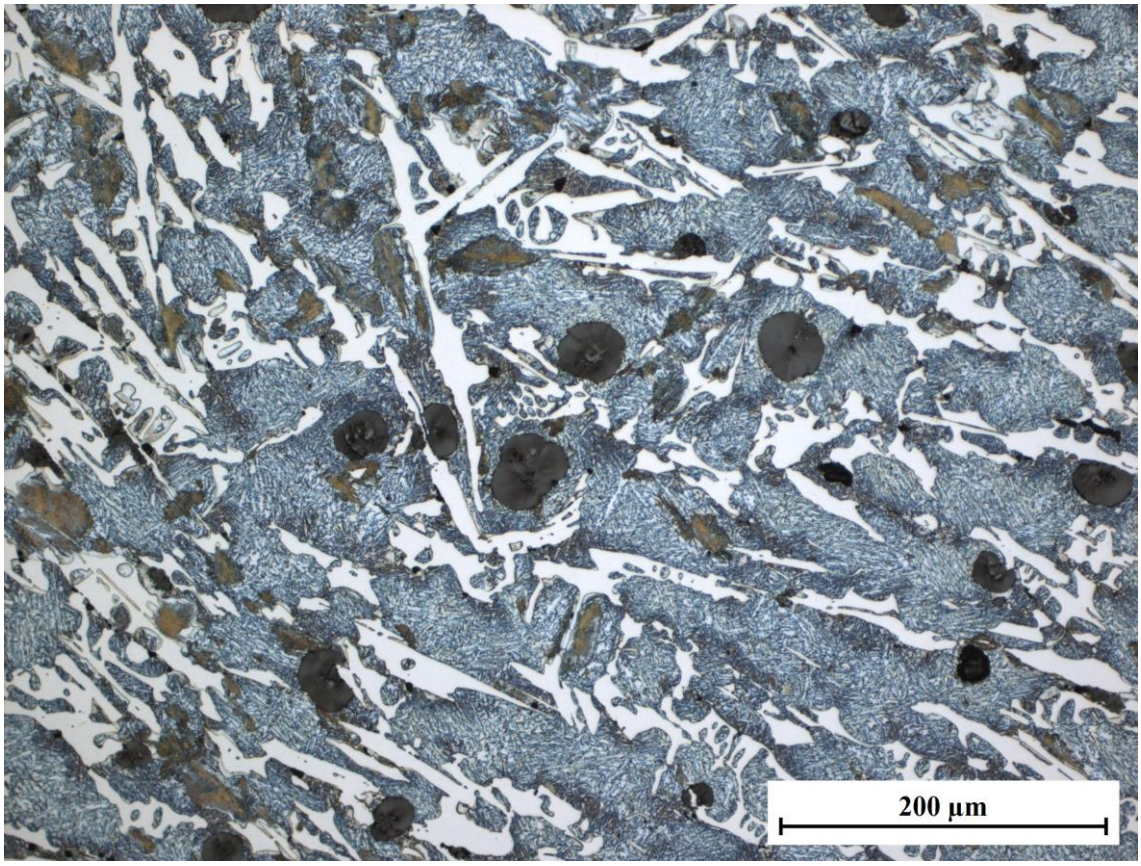

Figure 1. Microstructure of the reference material taken from a roll that broke under load with white primary carbides, black graphite, brown pearlite and blue bainite enclosing small white fields of retained austenite that did not transform (200x, etched with 3 % picric acid)

The challenge in designing a new bainitic-austenitic-martensitic-alloy is the complex interplay of alloying elements as material characteristics do not change proportionately to element content variation. There are mutual element interactions that influence bainite transformation kinetics [3]. Basically, the matrix evolution is influenced by controlling carbon diffusion that directly effects bainite growth [5]. Mainly, there are two sets of elements: those that lower bainite start temperature and

transformation time like Mn, Ni, Cr, and Si, and others that cause a distinct separation of pearlite and bainite region in the TTT-diagram (Cr, Mo, V, W) by forming a transformation inertial zone [3].

A high *carbon* content in the austenitic matrix leads to an increased amount of finer bainitic ferrite needles as the C-redistribution in C-saturated austenite is hindered and bainite transformation start retarded. At the same time, carbide formation from austenite is favored as a possibility of carbon storage [3].

Manganese stabilizes austenite and yields in longer bainite transformation times and the possibility of higher amounts of retained austenite when the reaction is interrupted too early [3], [6].

Nickel also lowers bainite start temperature, leading to a narrowed temperature region of bainite transformation [7].

Combined additions of molybdenum and nickel increase wear resistance and hardness as well as temperature stability especially if enough carbon is present. However, sulfur and phosphorous contents should be low in a material exposed to an environment of alternating temperature [8]. With 2.0 wt.% Mo and 0.5-1.0 wt.% Ni a mixture of upper and lower bainite can be obtained in cast iron; after austenite transformation finishes lower bainite is fully enclosed by upper bainite [9].

Chromium lowers bainite start temperature and retards transformation to such an extent that an inertial region between pearlite and bainite transformation zone can form [3].

In the need of avoiding the formation of ferrite and pearlite during quenching *molybdenum* can be of great advantage – especially in massive castings [3]. But it also delays the bainitic reaction, so longer treatment times or even incomplete transformation can be the consequence [6].

If *silicon* content is high (>2 wt.%), it can prevent carbide precipitation [6] in upper bainite (>350 °C) resulting in a matrix of bainitic ferrite and carbon-enriched austenite [10], [11]. Latter needs to be stabilized to prevent formation of martensite under load and the material becoming brittle [12], [13].

To develop a sufficed wear resistance for roll applications a sufficient number of carbides needs to be present. At the same time they must not grow too outstretched along grain boundaries as cracks develop along the primary carbide network when experiencing thermal fatigue or contact stresses or both [14].

This delicate combination of elements used for microstructure control is not easy to handle and the scattered use of trial and error does not necessarily lead to success. The most promising approach is the use of systematic design of elements (DoE) where the combination of well-selected element contents and resulting microstructure and mechanical properties is analyzed and used to find the perfect match for the application in focus.

2 Requirements and goal

The goal was the development of a new ductile cast iron for rolls with

- a bainitic-austenitic-martensitic microstructure replacing the wear-conventional pearlite-primary carbide mixture,
- exceeding the present properties of the reference material that failed in action with
  - yield strength > 830 N/mm² (covering thermal and mechanical stresses calculated in *Part 1: Simulation-based process characterization [15]*),
  - elongation min. 1 %, better 1.5 %,

- nodularity > 80 %,
- primary carbides (>2 %) to provide wear resistance, and
- hardness 350-450 HV30, more would reduce machinability of the material,

to face the alternating thermal and mechanical strain during the rolling of hot material and interjacent cooling periods.

Our approach to achieve these goals is to optimize the material by variation of nickel, molybdenum, and chromium in ductile iron.

3 Approach

Starting from the reference alloy (Table 1) crucial alloying elements are varied in the limits of

- *w*(Ni) = 2.0–2.5 %
- *w*(Mo) = 0.4-1.0 %
- *w*(Cr) = 0.1–0.4 %.

Table 1. Chemical composition of reference roll, starting melts, and input materials (mass fractions in percent)

	C	Cr	Mg	Mn	Mo	Ni	S	Si	Al	Ca	Ce/RE	Fe
reference roll	3.0	0.21	0.04	0.8	0.8	2.3	0.01	2.1	-	-	-	bal.
starting melt*	3.15	-	-	0.85	-	-	<0.05	1.75	-	-	-	bal.
nickel	-	-	-	-	-	≥ 98	-	-	-	-	-	-
FeSi	-	-	-	-	-	-	-	75	≤1	-	-	24
FeCr	7	65	-	-	-	-	-	-	-	-	-	28
FeMo	-	-	-	-	68	-	-	-	-	-	-	32
Mg-wire	18	-	26	-	-	-	-	14	-	-	1	bal.
inoculant	-	-	-	-	-	-	-	73	1	1	1.8	bal.

*before alloying with Ni, Mo, Cr, Mg treatment and inoculation

Following the approach of Design of Experiments (DoE) a full factorial experimental design is composed with 3 factors (Ni, Mo, Cr) in 2 levels (min/max content) yielding $2^3 = 8$ alloys (N1-N8) with 3 center points (N9-N11), for detection of non-linearities and for checking the reproducibility at median composition level, resulting in a set of 11 alloys summarized in Table 2.

Table 2. Set of 11 element variations from full factorial experimental design with center points N9-N11 (mass fractions in percent)

DoE N°	N1	N2	N3	N4	N5	N6	N7	N8	N9	N10	N11
nickel	2.00	2.50	2.00	2.50	2.00	2.50	2.00	2.50	2.25	2.00	2.50
molybdenum	0.40	0.40	1.00	1.00	0.40	0.40	1.00	1.00	0.70	0.40	0.40
chromium	0.10	0.10	0.10	0.10	0.40	0.40	0.40	0.40	0.25	0.10	0.10

The alloys were composed in a medium frequency induction furnace on a base of 5 % pig iron, 15 % cast iron return, and 80 % steel scrap. The base melt (Table 1) was alloyed with pure nickel and ferrous master alloys of silicon, chromium, and molybdenum to get the final composition. After then it was tapped at 1550 °C and treated with ferro-silicon magnesium wire and 0.3 % inoculant. It was cast with 1380 °C into a cylindrical iron chill and unpacked after solidification and cooling down to <300 °C. One roll has a weight of 820 kg.

After cooling and unpacking, all test rolls were cut to massive discs and heat-treated in a procedure following Table 3. From the finished material specimens were wire-eroded for characterization Figure 2.

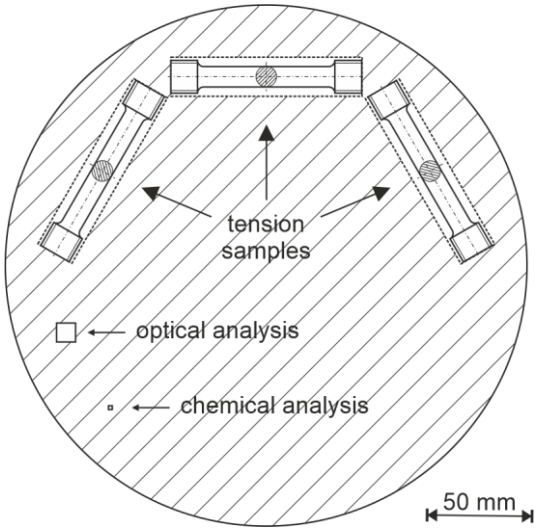

Figure 2. Specimen positions in heat-treated massive discs of 275 mm diameter (schematic)

Table 3. Steps and temperatures of heat treatment

step	temperature	duration
austenitizing	920 °C	75 min
quenching*	920-220 °C	163 min
annealing	>250 °C	90 min

*in multiple stages

4 Characterization

The investigation of all alloys includes wet-chemical analysis of composition via optical emission spectroscopy with inductively coupled plasma (DIN 51008-2), tensile tests following DIN 6892 and DIN 50125 form B (M12), Vickers hardness testing (DIN EN ISO 6507), and photo-optical analysis of microstructure including graphite characterization (ISO-TR 945-2) and quantitative phase analysis (point count ASTM E562).

The results from chemical analysis (Table 4 and Table 5) show sufficient accuracy in element content at final composition with regard to comparability to the reference material (Table 1) and in the element variation to fulfil the DoE target contents (Table 2).

Table 4. Final composition of alloys N1-11 of unvaried element contents (mass fraction in percent in chem. analysis samples)

	C	Cu	Mg	Mn	S	Si
final composition	3.09 ±0.13	0.11 ±0.02	0.03 ±0.01	0.68 ±0.21	0.02 ±0.00	1.99 ±0.08

Table 5. Final varied elements of alloys N1-11 (mass fraction in percent in chem. analysis samples)

DoE N°	N1	N2	N3	N4	N5	N6	N7	N8	N9	N10	N11
nickel	1.84	2.53	1.79	2.29	1.8	2.18	1.92	2.21	2.14	2.13	2.24
molybdenum	0.4	0.39	0.93	0.91	0.4	0.39	0.91	0.94	0.71	0.72	0.71
chromium	0.1	0.12	0.1	0.1	0.3	0.3	0.35	0.31	0.23	0.23	0.23

The results of mechanical characterization of all 11 alloys are summarized in Table 6. It is evident that all alloys fulfil the criterion of hardness values in the range of 350-450 HV30; only the alloys N5 and N8 fall below or exceed the specified interval. In addition, a mark of 830 N/mm² as maximum surface yield stress must be crossed – a detail the authors recommended from the rolling simulation in the first part of this paper with superposition of mechanical and thermal stresses [15]. The final position of the best alloy depends on the optimization of yield strength $R_{p0.2}$ and elongation $A_{5.65}$.

Table 6. Data from tensile and hardness testing

DoE N°	N1	N2	N3	N4	N5	N6	N7	N8	N9	N10	N11
R_m in N/mm²	943 ±3	1011 ±3	871 ±32	1003 ±13	925 ±1	911 ±3	878 ±10	837 ±5	971 ±5	976 ±3	952 ±3
$R_{p0.2}$ in N/mm²	762 ±12	812 ±4	754 ±5	830 ±1	812 ±3	852 ±2	839 ±2	815 ±7	816 ±2	804 ±7	825 ±6
$A_{5.65}$ in %	2.4 ±0.2	2.4 ±0.1	0.5 ±0.2	1.4 ±0.6	1.1 ±0.1	0.4 ±0.1	0.4 ±0.1	0.3 ±0.1	1.5 ±0.1	1.7 ±0.4	1.0 ±0.1
HV30	351 ±8	420 ±15	366 ±15	382 ±9	343 ±7	415 ±8	430 ±6	459 ±10	388 ±5	365 ±5	397 ±12

The characterization of microstructure (Table 7) revealed that nodularity is appropriate (>80 %) for all compositions except N1 which misses 3 %. Primary carbides are of sufficient number (>2 %) to provide enough wear resistance. On the other hand, carbide and martensite fractions should be low enough to keep a ductile, non-brittle matrix. At the same time, the matrix needs to be strong, achieved by formation of bainite.

Table 7. Data from microstructural characterization (all values in %, rest max. 3 % primary ferrite/austenite)

DoE N°	N1	N2	N3	N4	N5	N6	N7	N8	N9	N10	N11
graphite	7.2	9.3	7.9	8.8	8.6	9.3	7.0	7.9	6.9	5.4	6.4
nodularity	77.0	92.2	94.0	85.0	89.6	90.2	86.5	85.7	90.3	76.8	83.8
bainite	52.5	9.0	7.0	25.7	56.0	38.4	29.9	17.6	1.4	3.1	4.1
primary carbides	5.0	4.9	6.8	7.5	6.4	1.7	6.2	10.9	10.8	10.7	7.9
pearlite	3.7	0.0	2.4	0.0	0.2	0.0	9.0	4.6	3.8	1.0	2.0
martensite	28.3	73.7	75.5	58.1	28.8	50.6	45.7	58.0	76.8	79.9	79.1

This apparent contradiction is solved by unfolding the changing material characteristics in the design space framed by the composition ranges of nickel, molybdenum, and chromium. The combination of mathematical correlations describing the course of properties and restricting conditions leads to an ideal alloy composition. This approach is the ultimate target of DoE and is described in the following chapter.

5 Statistical experiment evaluation

All empirical data was entered into the statistical evaluation and subjected to a regression analysis. The highest possible model quality should be strived. A good model would have a model fit $R^2 > 0.7$, an estimate of the future prediction precision of $Q^2 > 0.5$, a model validity > 0.25, and a reproducibility > 0.5 to show the variation of the replicates (N9-N11) compared to the overall variability. The following mathematical correlations for the mechanical properties were found:

$R_{p0.2} = (608 + 75 \cdot w(\text{Ni}) + 214 \cdot w(\text{Cr}))$ N/mm²

$A = (4.2 + 0.3 \cdot w(\text{Ni}) - 3.8 \cdot w(\text{Mo}) - 12.1 \cdot w(\text{Cr}) - 10.6 \cdot w(\text{Mo}) \cdot w(\text{Cr}))$ %

$HV = (391 + 16 \cdot w(\text{Ni}) + 11 \cdot w(\text{Mo}) + 18 \cdot w(\text{Cr}) - 8\, w(\text{Ni}) \cdot w(\text{Mo}) + 11 \cdot w(\text{Mo}) \cdot w(\text{Cr}))$ HV30

These equations describe the empirical data quite sufficiently. Table 8 gives an overview of their model qualities. Every parameter reaches the minimum requirements of a good model, only the future prediction precision of elongation is at the lower limit.

Table 8. Model quality for tensile strength R_m, yield strength $R_{p0.2}$, elongation A, and hardness HV

	$R_{p0.2}$	A	HV
model fit R^2	0.736	0.777	0.800
future prediction precision Q^2	0.613	0.495	0.526
validity	0.471	0.767	0.618
reproducibility	0.945	0.752	0.849

To identify the Sweet Spot region that includes the optimal alloy a combination of alloy requirements (conditions) and mathematical correlations is needed. The necessary and essential requirements derived from the simulation approach from the first paper and the broken reference roll are

- $R_{p0.2} > 830$ N/mm²,
- $A > 1.5$ %, and
- $HV = 350$-450 HV30.

All these conditions are fulfilled in the red area in Figure 3.

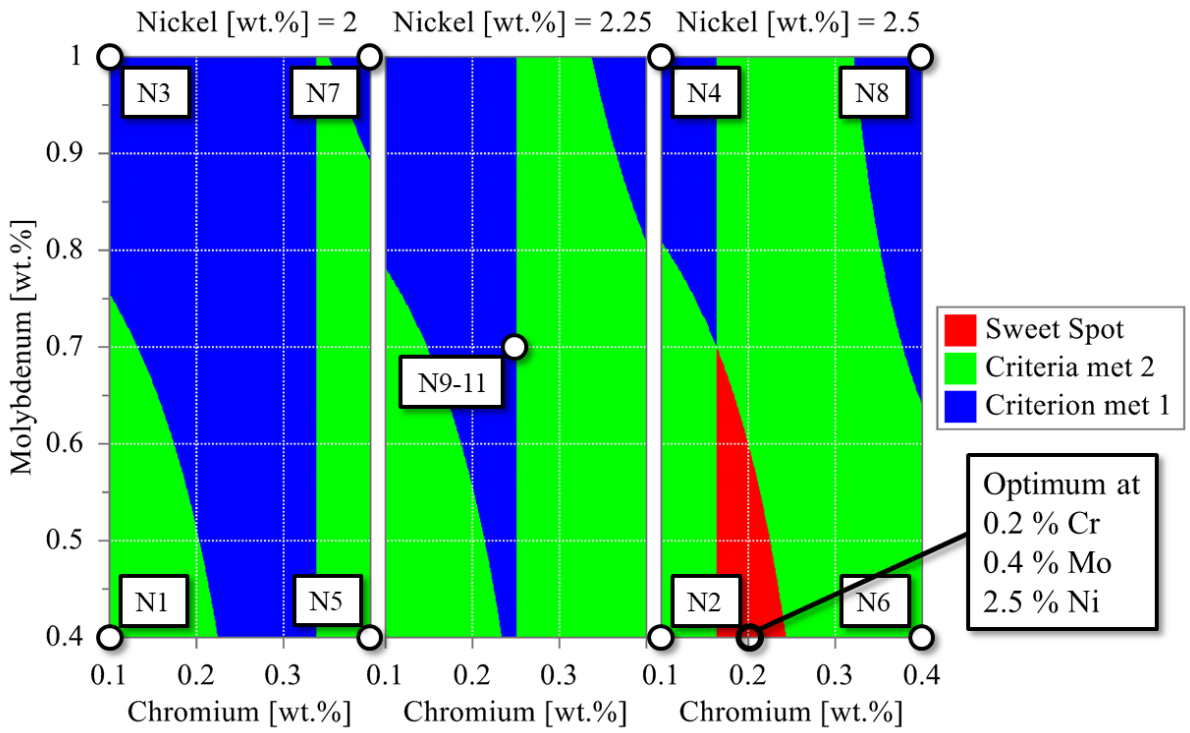

Figure 3. Sweet Spot Plot resulting from combination of mathematical models and alloy requirements (criteria $R_{p0.2}$ > 830 N/mm², A = >1.5 %, HV = 350-450 HV30)

For the selection of the new, optimized alloy the decision criteria were:

- The **molybdenum** content is determined to the lower limit of **0.4 wt.%** for cost reasons.
- The **chromium** content should be around **0.2 wt.%** to allow for manufacturing tolerances.
- The **nickel** content with **2.5 wt.%** is fixed.

6 Model validation

A validation of the mathematical models was done using the parameters of the Sweet Spot alloy. The optimum alloy with 0.4 wt.% Mo, 0.2 wt.% Cr, and 2.5 wt.% Ni was cast into the same iron chill as the previous alloys N1-N11. This time the heat treatment was done at small scale with a single disc in the laboratory furnace for practical reasons. Subsequently, specimens were cut and characterized following the same procedure as before.

Looking at the results, the Sweet Spot alloy fulfils the project requirements of yield strength and hardness as proposed in the beginning (target areas in Figure 4). However, a comparison of empirical values and data calculated for the cast Sweet Spot composition using the equations stated above revealed deviations that needed an investigation.

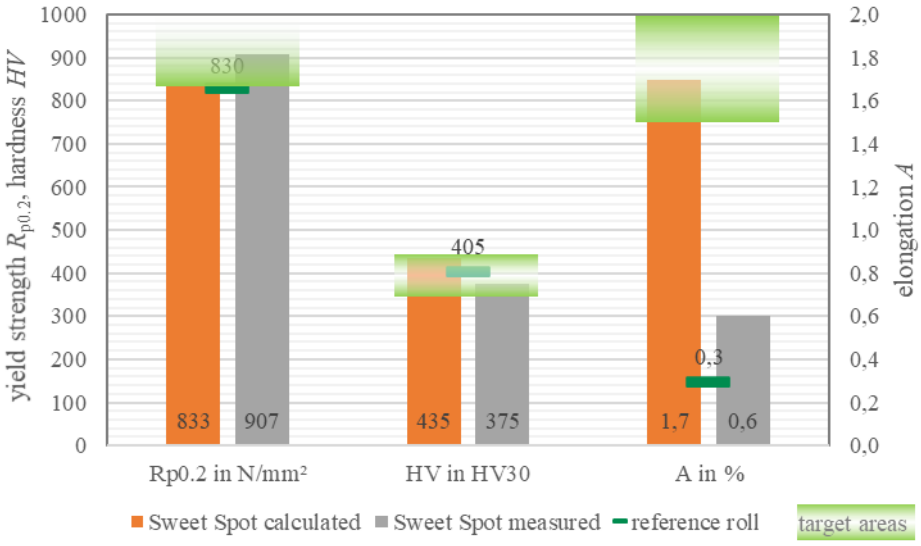

Figure 4. Graphical comparison of the calculated and empirical mechanical properties of the Sweet Spot alloy, including the required properties (target areas) and the data of the broken reference roll

Figure 4 shows: The Sweet Spot alloy's yield strength $R_{p0.2}$ is 74 N/mm² above the calculated value (prediction precision $Q_2 = 0.613$), elongation at break is -1.1 % off ($Q_2 = 0.495$), measured and calculated hardness difference goes into the same direction ($Q_2 = 0.526$). All in all, the future prediction precision seems not to be sufficient. Especially the strong deviation of the real elongation at fracture stood out. Consequently, a microstructural analysis was carried out on one the tensile specimens tested here (sample taken from thread-part). This led to the explanation: the microstructure was composed slightly differently (Figure 5). There is a significantly higher proportion of retained austenite in the bainitic matrix (white fields in between ferrite needles) that did not undergo the transformation to bainite. This explains the lower hardness measured. Not stabilized, the high carbon retained austenite converts to martensite under load (during the tensile test), strengthens the material and diminishes the elongation [10], [13], [16]. This would be the reason for the excess yield strength and the insufficient elongation at break. The explanation for this change in microstructure lies in the slightly different heat treatment of the Sweet Spot alloy. On industrial scale heat treatment, the discs of alloys N1-N11 were positioned next to each other in a way that a mutual influence during cooling periods cannot be denied. So, it is possible that more time at elevated temperature was gained to complete the bainitic transformation. In laboratory scale the disc was surrounded by cooler air. This leaves room for the possibility of an interrupted bainitic transformation yielding in retained austenite. Nevertheless, aside from hardness being a little low, the new alloy outmatches the broken reference roll as undoubtedly presented in Figure 4.

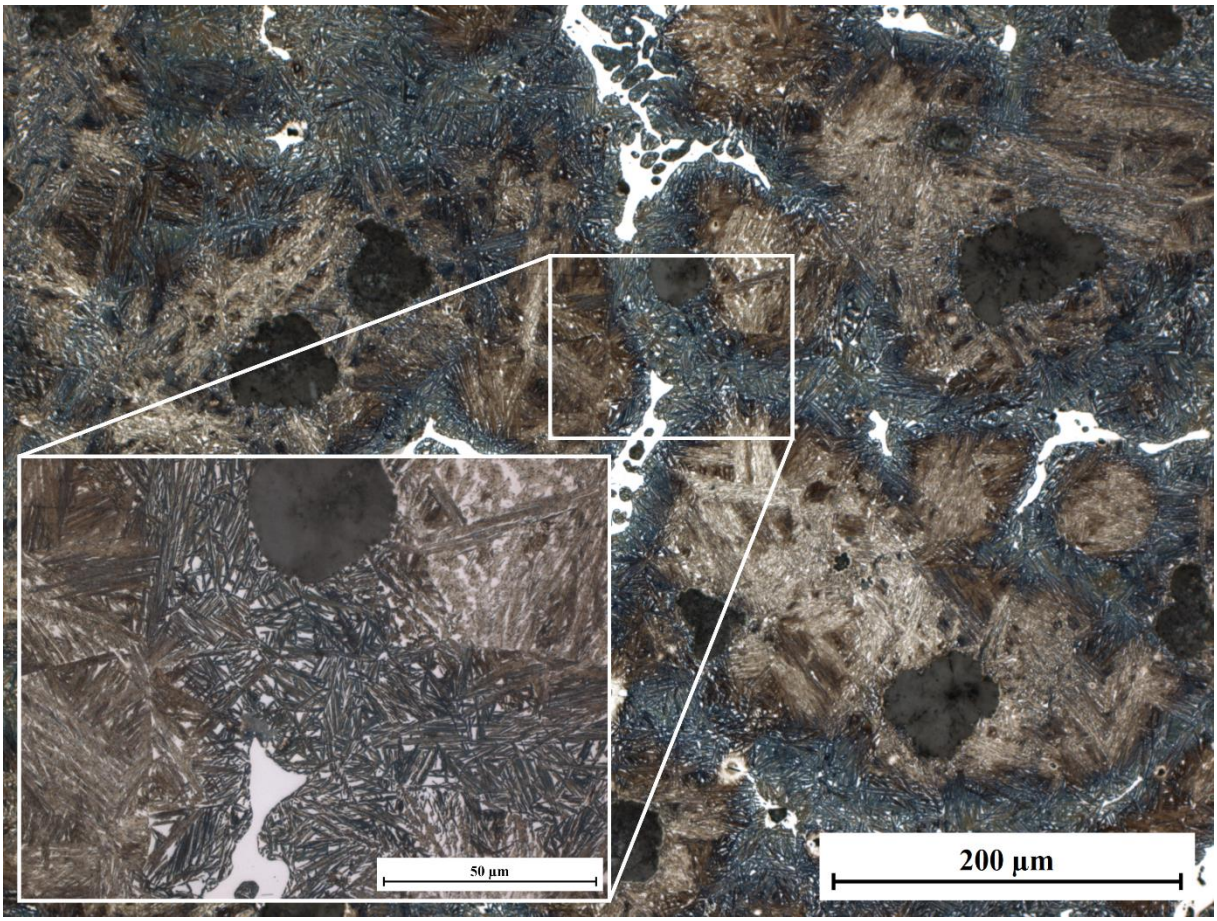

Figure 5. Tensile test specimen of Sweet Spot alloy: bainitic matrix with ferrite needles (brown/blue), retained austenite (white, between needles), graphite nodules, and white Fe_3C/Mo-carbides (200x and 1000x, etched with Beraha I)

In the end, the conclusion can be drawn that mathematical modelling is feasible and can deliver good results. However, if retained austenite is present it needs to be stabilized so that the material's microstructure does not change during characterization.

7 Findings & Conclusion

The creation of models based on the empirical data obtained was successful. A validation of the mathematical equations set up by the optimized alloy resulted in relative deviations of a maximum of 14 % in the mechanical characteristic values. The only exception was the elongation at break. The reason for this was a different microstructure resulting from a change of scale in heat treatment. The Sweet Spot tensile samples underwent an interrupted bainitic transformation that yielded in retained austenite and finally martensitic embrittlement. This fine change must be considered in future investigations. An implementation of microstructure/heat treatment interaction into the mathematical modelling is imaginable. In this way, the interplay of characteristic values and quality of mathematical models can be improved even further and allows exact predictions of the mechanical properties and microstructural compositions of newly developed alloys.

Acknowledgments

The Federal Ministry for Economic Affairs and Energy supported this work under Grant N° ZF4506901.

Declaration of interest statement

The authors reported no potential conflict of interest.

[1] Gumienny G (2013) *Effect of the Carbides and Matrix on the Wear Resistance of Nodular Cast Iron.* Archives of Foundry Engineering 13: 25–29.

[2] Cui J, Zhang H, et al. (2014) *Microstructure and Mechanical Properties of a Wear-Resistant As-Cast Alloyed Bainite Ductile Iron.* Acta Metall. Sin. (Engl. Lett.) 27: 476–482.

[3] Lünenbürger A (1991) *Zum Umwandlungs- und Verformungsverhalten bainitisch-austenitischer Siliziumstähle,* Karlsruhe, Dissertation.

[4] Saikoff E, Andersson E, Bengtsson F, Olausen C, Galstyan M, Vikström D, Lazraq Byström J (2018) *Cobalt in high speed steels,* Uppsala, Independent bachelor thesis.

[5] Mehl R F (1938) *The physics of hardenability,* Detroit.

[6] Benam A S (2015) *Effect of alloying elements on austempered ductile iron (ADI) properties and its process: Review.* China Foundry 12: 54–70.

[7] Bhadeshia H K D H (2005) *52nd Hatfield Memorial Lecture Large chunks of very strong steel.* Mater. Sci. Technol. 21: 1293–1302.

[8] Bunin K P, Troizkaja E P, Citrik S N (1945) *Einfluss einzelner Elemente auf die thermische Beständigkeit (Stabilität) von weißem Gußeisen.* Stal' 5: 417–419.

[9] Pietrowski S, Gumienny G (2010) *Bainite obtaining in cast iron with carbides castings.* Archives of Foundry Engineering 10: 109–114.

[10] Sandvik B P J, Nevalainen H P (1981) *Structure-property relationships in commercial low-alloy bainitic-austenitic steel with high strength, ductility, and toughness.* Met. Technol. 8: 213–220.

[11] Kozeschnik E, Bhadeshia H K D H (2008) *Influence of silicon on cementite precipitation in steels.* Mater. Sci. Technol. 24: 343–347.

[12] Bhadeshia H K D H, Edmonds D V (1983) *Bainite in Silicon Steels: A New Composition-Property approach. Part I.* Metal Science 17: 411–419.

[13] Bhadeshia H K D H (2010) *Nanostructured bainite.* Proc. R. Soc. A. 466: 3–18.

[14] Colás R, Ramírez J, et al. (1999) *Damage in hot rolling work rolls.* Wear 230: 56–60.

[15] Liepe M, Duwe S, et al. ((to be published)) *A new Ductile Iron for mechanically and thermally strained rolls*: *Part 1: Simulation-based process characterization of hot rolling.* Int. J. Cast Metal. Res.

[16] Schaaber O (1952) *Über Einflussfaktoren bei der isothermen Austenitumwandlung in der Zwischenstufe (Bainitgebiet I und II).* Draht: 7–13.